SATELLITE DERIVED COASTAL WATER BATHYMETRY: IMPLICATIONS AND APPLICABILITY OF SPATIAL HOMOGENEITY ASSUMPTION

Ryan Tan*[1], Rakesh Kumar Singh[1], Amihan Manuel[1] and Soo Chin Liew[1]
[1]Centre for Remote Imaging, Sensing and Processing (CRISP), National University of Singapore, Singapore - 119076
Email: tanryan@nus.edu.sg*, rakesh.singh@nus.edu.sg, aymanuel@nus.edu.sg, scliew@nus.edu.sg

KEY WORDS : Bathymetry, Coastal waters, Sentinel-2, Spatial Homogeneity

ABSTRACT : Bathymetry of oceans, seas, and lakes is essential for the navigation of ships, planning of offshore infrastructure, marine environment monitoring, and several other applications. Satellite-derived bathymetry has become more prevalently used due to its cost-effectiveness, wide coverage, and convenience of data retrieval and integration. This paper analyses a method to estimate the bathymetry of coastal waters based on the assumption of spatial homogeneity (ASH) in the optical properties of the surrounding deep waters and investigates its accuracy at varying turbidity. The area of interest for this study is Singapore where the coastal waters are shallow, dynamic, and turbid. Data retrieved from Sentinel-2 were processed at 10m resolution and the results were then validated with the data extracted from electronic navigational charts. Our study showed that bathymetry obtained through ASH of coastal and deep waters has diminishing accuracy in regions where turbidity is higher. However, by adjusting the extent of the region assumed to be homogenous according to the turbidity of the coastal areas, the bathymetry can be estimated with significant accuracy using ASH.

1 INTRODUCTION

Satellite-derived methods of bathymetry make use of remotely sensed reflectance of seawater to estimate the water depths by performing physical calculations. However, remotely sensed data using optical bands are subjected to inaccuracies in waters that are shallow and highly turbid [1, 2]. To account for this, validation with other sources of data such as field observations is also usually done to substantiate the results from satellite-derived bathymetry. However, field observations are usually costly and labour-intensive, thus, we want to perform cost-effective validation by performing tests on the physical model and with the help of Electronic Navigation Charts (ENCs) which are easily obtainable. ASH is a method of estimating the reflectance of coastal waters based on the assumption of the homogenous properties of water between the shallow and the deep regions. This is based on the presumption that the deep waters are close enough to the shallow waters such that their optical properties are the same. This assumption is usually valid for waters that are clear and calm but becomes less accurate where the waters contain many suspended particles moving around [3]. Hence, we aim to explore this assumption and the extent to which it holds true.

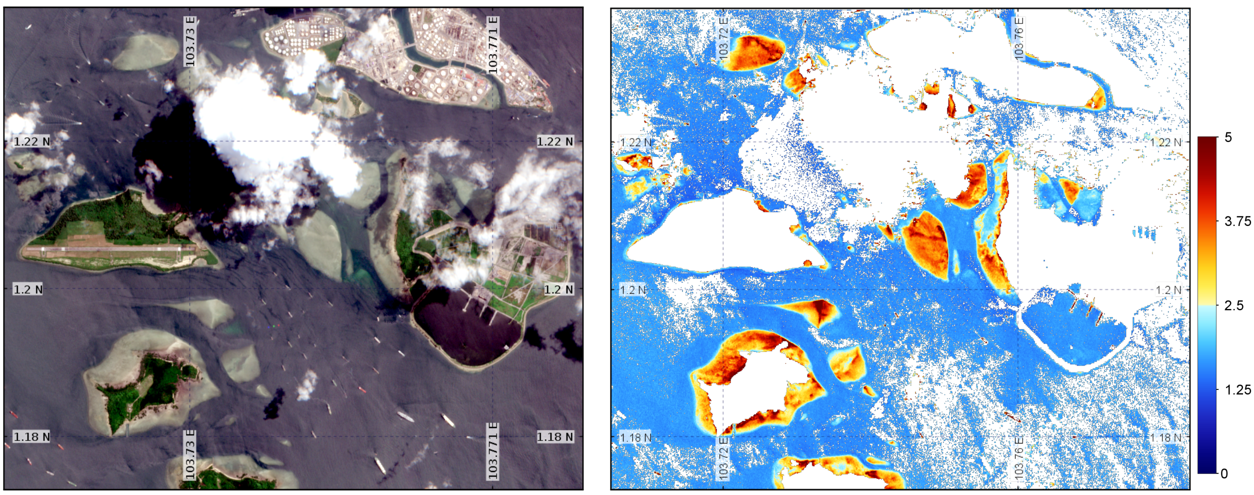

(a) True colour image of AOI

(b) Diffused attenuation coefficient at 490 nm ($K_\mathrm{d}(490\mathrm{nm})$) of AOI. Note that the unit of $K_\mathrm{d}(\lambda)$ is m^{-1} and white areas are masked out

Figure 1: Area of interest

2 STUDY AREA

The study area is Singapore, in particular, the area of interest (AOI) is the small area around the southern islands of Singapore. One image tile dated 8th August 2023 was acquired from Sentinel-2 MultiSpectral Imager (MSI) as seen from the True colour image in Figure 1(a). The MSI image is retrieved as level 1C top of atmosphere (TOA) radiance and atmospherically corrected and resampled to 10-m resolution. It is then subsequently used to calculate the bathymetry and the diffused attenuation coefficient of the AOI at 490 nm ($K_{\mathrm{d}}(490\mathrm{nm})$) as shown in Figure 1(b).

3 METHOD

The images retrieved from Sentinel-2 MSI level 1C TOA radiances, $L_{\mathrm{TOA}}(\lambda)$ are converted to TOA reflectance $R_{\mathrm{TOA}}(\lambda)$ by the following equation:

$$R_{\mathrm{TOA}}(\lambda) = \frac{\pi L_{\mathrm{TOA}}(\lambda)}{d^2 F(\lambda)\cos\theta_{\mathrm{s}}} \tag{1}$$

where d^2 is the correction factor for the solar irradiance due to the varying Earth-Sun distance at different times of the year, $F(\lambda)$ is the average solar flux density, and θ_{s} the solar zenith angle.

The absolute radiometric uncertainty of Sentinel-2 MSI level 1C products is very stable at less than $3\% \pm 2\%$ and the signal-to-noise ratio (SNR) of all bands has more than 27% margin compliant with the requirement [4]. The TOA reflectance is also atmospheric corrected for scattering by air molecules and aerosols, and absorption using NASA's SeaDAS [5] to get the surface remote sensing reflectance, $R_{\mathrm{rs}}(\lambda)$. A basic method to remove the sun glint from the images was also done by subtracting the reflectance of the near-infrared (NIR) band multiplied by an aerosol factor [6]. This is based on the assumption that the aerosol path reflectance is spectrally flat. Hence, with the surface reflectance, we can get the subsurface reflectance by [7]

$$r_{\mathrm{rs}}(\lambda) = \frac{R_{\mathrm{rs}}(\lambda)}{0.52 + 1.7R_{\mathrm{rs}}(\lambda)} \tag{2}$$

which can also be expressed as [7]

$$r_{\mathrm{rs}}(\lambda) = r_{\mathrm{w}}(\lambda)(1 - e^{-K_{\mathrm{d}}(\lambda)MH}) + r_b(\lambda)e^{-K_{\mathrm{d}}(\lambda)MH} \tag{3}$$

where r_{b} is the bottom albedo, $r_{\mathrm{w}}(\lambda)$ is the reflectance from deep waters, $K_{\mathrm{d}}(\lambda)$ is the attenuation coefficient, H is the water depth and M is computed as

$$M = 1/\cos\theta_{\mathrm{v}} + 1/\cos\theta_{\mathrm{s}} \tag{4}$$

where θ_{v} and θ_{s} are the subsurface viewing and solar zenith angles respectively.

To get the subsurface deep water reflectance here, we employ the method of ASH. Hence, they are retrieved from deep water areas that are surrounding coastal waters. The subsurface deep water reflectance can be expressed as [8]

$$r_{\mathrm{w}}(\lambda) = \frac{0.33b_{\mathrm{b}}(\lambda)}{K_{\mathrm{d}}(\lambda)} \tag{5}$$

$$K_{\mathrm{d}}(\lambda) \approx a(\lambda) + b_{\mathrm{b}}(\lambda) \tag{6}$$

where $a(\lambda)$ and $b_{\mathrm{b}}(\lambda)$ are the absorption and backscattering coefficients of the deep waters which can be calculated using a quasi-analytical algorithm (QAA) [9, 10].

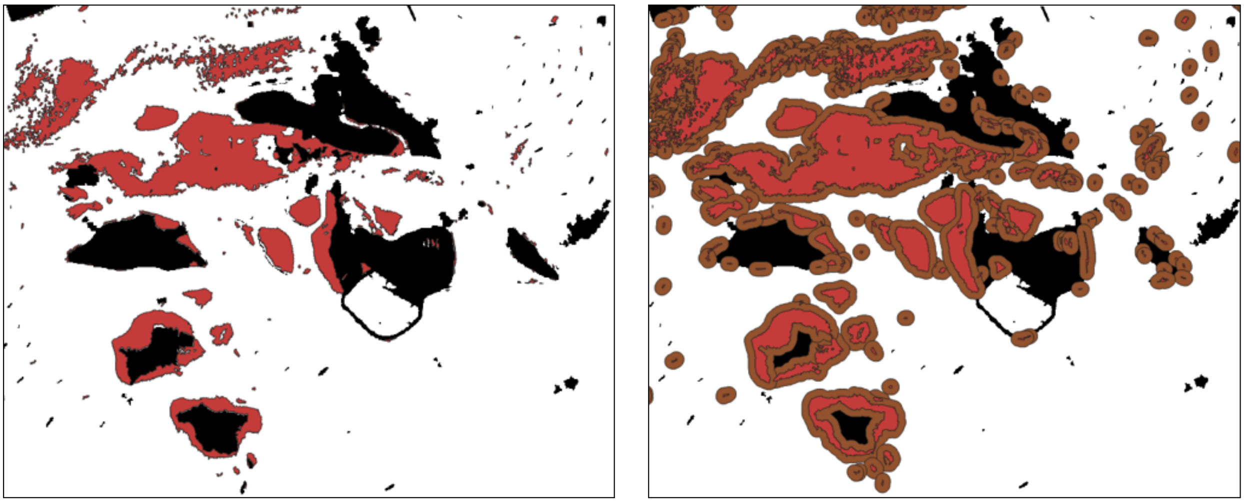

(a) Shallow water polygons (red). Black regions denote land and ships, while the white region is identified as optically deep waters.

(b) Expanded of polygons (brown) showing the region selected to pick $r_{\mathrm{w}}(\lambda)$ values.

Figure 2: Shallow water polygons and expansion

Figure 2 above shows some of the shallow water regions in Singapore which are identified via classification and converted to shape polygons as seen in Figure 2(a). The red polygons represent pixels that are identified as shallow water and the white regions represent pixels that are identified as deep. Subsequently, the shallow water polygons are expanded by a certain number of pixels (1 pixel = 10 meters) surrounding the shallow water polygons to retrieve the average of the surrounding deep water pixels. These deep water pixel averages are then used to compute the deep water reflectance, $r_{\mathrm{w}}(\lambda)$ based on ASH. In Figure 2(b), the expansion of 150 meters (15 pixels) is shown as an example. Varying the expansion size of the polygon will help us to determine the extent to which ASH can hold true as the further the deep waters are from the coastal waters, the less likely they will have the same optical properties, especially in turbid areas such as our AOI. With this we can obtain $r_{\mathrm{w}}(\lambda)$, then, H and r_{b} can be solved numerically.

4 RESULTS

The bathymetry is computed for 6 expansion sizes (10m, 50m, 90m, 150m, 200m, 280m), and a normalized bathymetry for all of them is shown in Figure 3. They are normalized by the maximum of the 6 bathymetry values for the ease of comparison between them and the color bar ranges from 0.8 to 1. The higher the normalized value, the higher the depth computed for the expansion size for the area. The bathymetry is computed for 6 expansion sizes (10m, 50m, 90m, 150m, 200m, 280m), and a normalized bathymetry for all of them is shown in Figure 3. They are normalized by the maximum of the 6 bathymetry values for the ease of comparison between them and the color bar ranges from 0.8 to 1. The higher the normalized value, the higher the depth computed for the expansion size for the area. Based on a comparison of the 6 images in Figure 3, we can see that the bathymetry for the 10m expansion is computing higher depth values in areas that are supposedly shallow (refer to Figure 1 for shallow and deep water areas) and lower depth values for regions that are supposedly deep. As the expansion size increases, initially the depth values computed get closer to the expected values for both the shallow and deep regions then again start to deviate until the 280m expansion is reached. For the 280m expansion, we can see that although the shallow regions are computed with lower depth values, the deeper regions are getting shallower. Hence, the best size for the polygon expansion should lie between 10m and 280m.

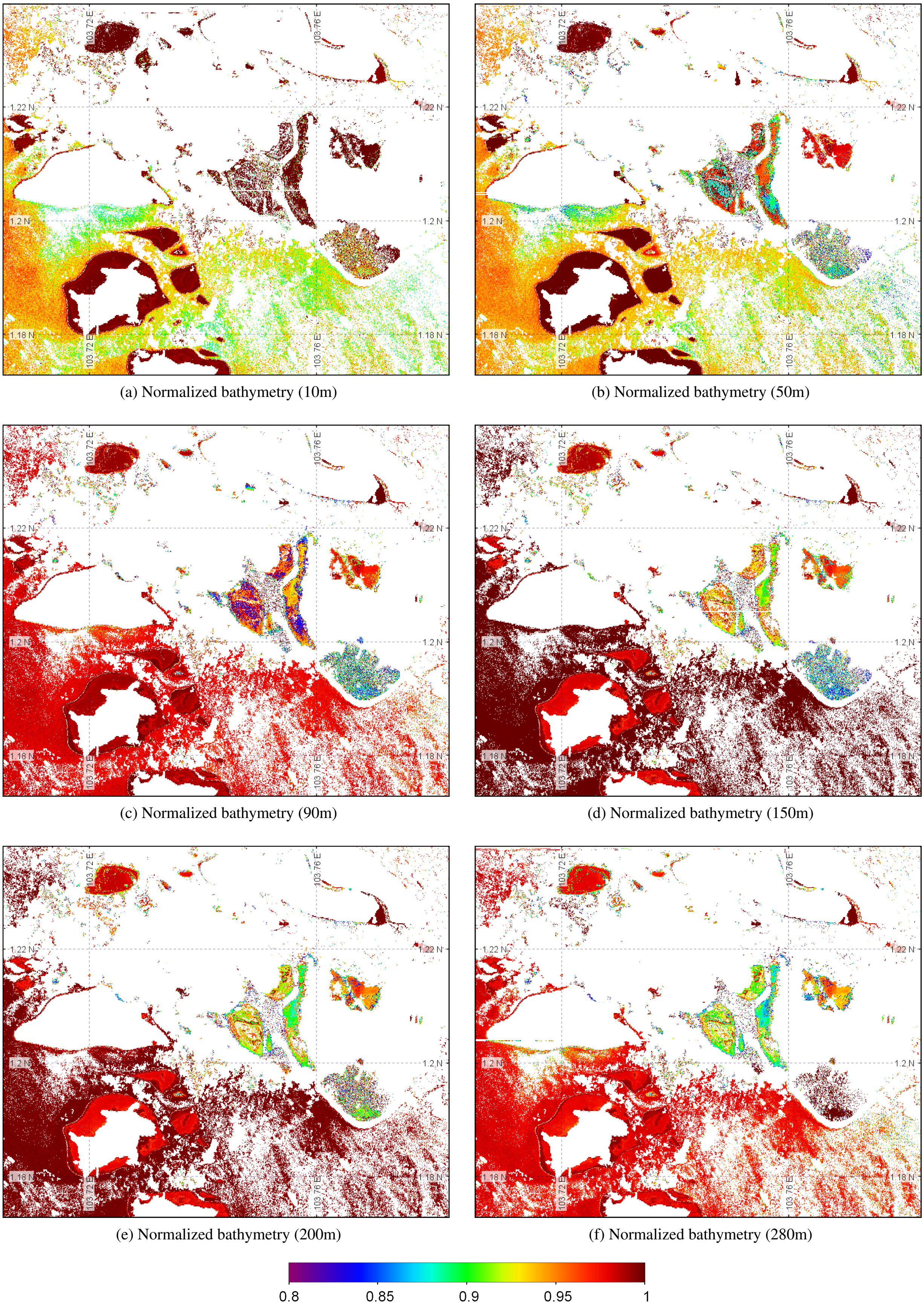

Figure 3: Variation of normalized bathymetry results for different polygon expansion sizes.

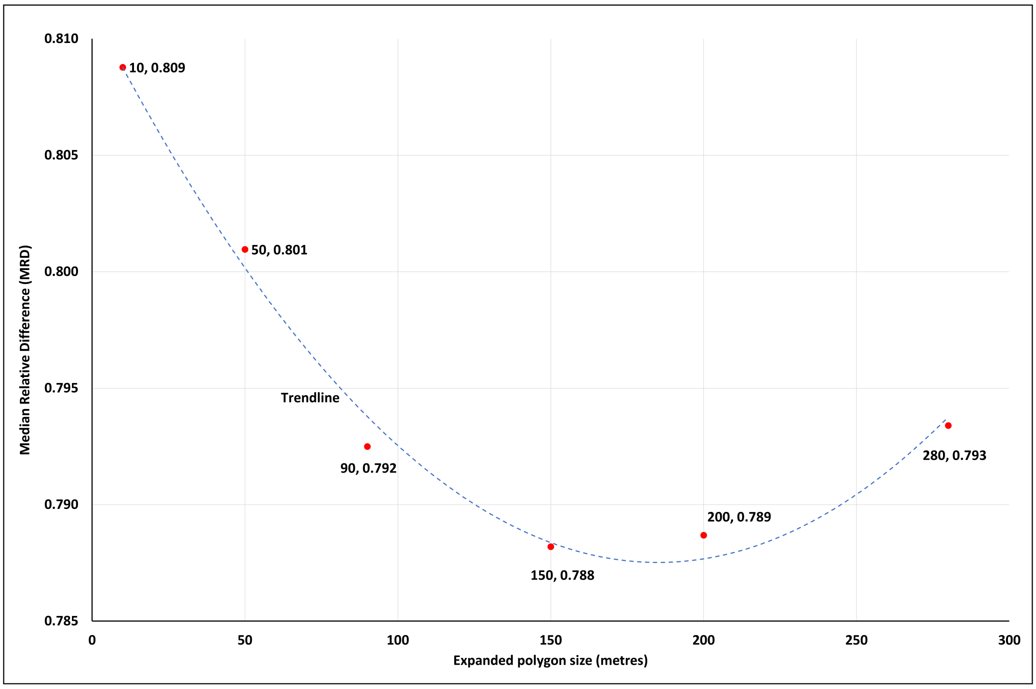

Figure 4: Median Relative Difference (MRD) computed for bathymetry products estimated using different expansion sizes.

To corroborate these results, we used depth points from Electronic Navigation Charts (ENCs) of Singapore obtained from ADMIRALTY Vector Chart Service (AVCS) [11]. Using ENC bathymetry as true values, we estimated the median relative difference (MRD) for all test cases and plotted in Fig. 4. It shows a decreasing MRD as the expansion size increases from 10m and has the lowest MRD for the 150m expansion before increasing again as the expansion gets higher. The high MRD (above 0.78) obtained for the results is expected due to the high amount of glint in the image as well as high turbidity in the coastal areas. In addition, as the coastal waters are generally very shallow (less than 1m) in depth, a small difference in the computed depth will result in high MRD values.

5 CONCLUSION

In this paper, we obtain the bathymetry results of a turbid area in Singapore waters using ASH between shallow and deep waters. The bathymetry is calculated using the remote sensing reflectance from the satellite image and the variation of 6 polygon sizes is done to test the extent of accuracy for which ASH holds true. By comparing the 6 different bathymetry results and using the MRD against ENC charts, our results indicate that the expansion size of about 150m gave the most accurate results in estimating bathymetry using ASH for turbid areas. However, we obtain relatively high MRD values across all the results which can perhaps be reduced by obtaining the mean bathymetry of a set of images of the same area over a time period [12]. The ASH between shallow and deep water still holds true in turbid waters, provided the area extent assumed to be homogeneous is not too big or small. This will allow us to further fine-tune similar existing analytical bathymetry models by choosing the optimal area extent around different types of water to achieve more accurate bathymetry results.

REFERENCES

[1] Isabel Caballero and Richard P Stumpf. Confronting turbidity, the major challenge for satellite-derived coastal bathymetry. *Science of the Total Environment*, 870:161898, 2023.

[2] SSJD Mudiyanselage, A Abd-Elrahman, B Wilkinson, and V Lecours. Satellite-derived bathymetry using machine learning and optimal Sentinel-2 imagery in South-West Florida coastal waters. *GIScience & Remote Sensing*, 59(1):1143–1158, 2022.

[3] Hubert Loisel, Vincent Vantrepotte, Cédric Jamet, and D Ngoc Dat. Challenges and new advances in ocean color remote sensing of coastal waters. *Topics in Oceanography*, pages 1–38, 2013.

[4] S2 MSI ESL team. Data Quality Report Sentinel-2 L1C MSI January 2023. *Sentinel Online*, 2023.

[5] Curtis D Mobley, Jeremy Werdell, Bryan Franz, Ziauddin Ahmad, and Sean Bailey. Atmospheric correction for satellite ocean color radiometry. Technical report, 2016.

[6] A Wang-Cheng Heng, Soo Chin Liew, and Chew Wai Chang. Retrieval of inherent optical properties from Landsat ETM+ data: possibilities and limitations. In *IGARSS 2004. 2004 IEEE International Geoscience and Remote Sensing Symposium*, volume 5, pages 3487–3488. IEEE, 2004.

[7] Zhongping Lee, Kendall L Carder, Curtis D Mobley, Robert G Steward, and Jennifer S Patch. Hyperspectral remote sensing for shallow waters: 2. Deriving bottom depths and water properties by optimization. *Applied optics*, 38(18):3831–3843, 1999.

[8] Howard R Gordon, Otis B Brown, and Michael M Jacobs. Computed relationships between the inherent and apparent optical properties of a flat homogeneous ocean. *Applied optics*, 14(2):417–427, 1975.

[9] ZhongPing Lee, Kendall L Carder, and Robert A Arnone. Deriving inherent optical properties from water color: a multiband quasi-analytical algorithm for optically deep waters. *Applied optics*, 41(27):5755–5772, 2002.

[10] Soo Chin Liew and Jiangcheng He. Uplift of a coral island in the andaman sea due to the 2004 sumatra earthquake measured using remote sensing reflectance of water. *IEEE Geoscience and Remote Sensing Letters*, 5(4):701–704, 2008.

[11] Vaughan Nail. A First Generation ENC Services. *The International Hydrographic Review*, 2010.

[12] Bertrand Lubac, Olivier Burvingt, Alexandre Nicolae Lerma, and Nadia Sénéchal. Performance and uncertainty of satellite-derived bathymetry empirical approaches in an energetic coastal environment. *Remote Sensing*, 14(10):2350, 2022.